Available online at www.sciencedirect.com

SciVerse ScienceDirect

Procedia CIRP 8 (2013) 39 – 44

www.elsevier.com/locate/procedia

14th CIRP Conference on Modeling of Machining Operations (CIRP CMMO)

Modeling deformations of the workpiece and removal of material when turning

S. Schindler[a,]*, M. Zimmermann[b], J.C. Aurich[b], P. Steinmann[a]

[a]*University of Erlangen Nuremberg, Chair of Applied Mechanics, Egerlandstr. 5, 91058 Erlangen City and Postcode*, Germany
[b]*University of Kaiserslautern, Institute for Manufacturing Technology and Production Systems, Gottlieb-Daimler-Str., 67663 Kaiserslautern*, Germany
* Corresponding author. Tel.: +49-9131-8528506; fax: +49-9131-8528503.*E-mail address*: Stefan.Schindler@ltm.uni-erlangen.de.

Abstract

During machining mechanical energy is dissipated into heat by frictional processes and plastic deformations of the workpiece material. Workpiece and tool are thereby subjected to thermal and mechanical loads that cause thermal expansions and mechanical deformations. These decrease the accuracy of machining. In order to reduce such deformations, enhanced cutting conditions need to be determined. Finite element (FE) simulations allow for such an optimization prior to actual machining. A validated 3D FE model to determine the temperature distribution and the deformations of the workpiece regarding the cutting condition and the actual tool position is outlined for turning. The continuous removal of material for arbitrary geometries when simulating the temperature distribution and the deformations is considered. This allows for the calculation of the actual workpiece diameter after turning.

Keywords: finite element simulation; temperature distribution; removal of material; deformations of the workpiece

1. Introduction

Approximately all mechanical work done when machining is converted into heat by the plastic deformation of the workpiece material and friction. Using dry cutting, the generated heat flows into the tool, the workpiece, and the chips. Tool, workpiece, and machine tool are hence subjected to mechanical and thermal loads. These loads that deform the tool, and the machine tool - workpiece system cause deviations between the nominal and the actual depth of cut. Such deviations decrease the accuracy of machining [1-3].

Increased demands on the precision of chip removal require a holistic consideration of machining in order to achieve these demands [4]. The deformations of the workpiece attained significance in recent years due to the increased use of dry cutting, particularly when turning [5-7]. Dry cutting raises the thermal loads on the workpiece because of the greater friction work and the not removed quantity of heat through the coolant. Thermal expansions of the workpiece are remarkably increased. Besides these thermally induced deformations, the workpiece is deflected by the process forces when turning. This additionally influences the actual depth of cut. In order to decrease or compensate such effects, the deformations of the workpiece need to be determined regarding the cutting condition and the actual tool position. Finite element simulations allow for this determination [8-10].

This paper presents a technique to calculate thermo-mechanical effects on the deformation of the workpiece. A 3D FE model of the workpiece determines the temperature distribution in the workpiece as well as its deformations and represents the removal of material. Cutting conditions can therefore be virtually optimized prior to actual turning in order to enhance the accuracy of machining.

doi:10.1016/j.procir.2013.06.062

2. Experimental design

Dry cutting investigations were carried out on a CNC lathe using polycrystalline diamond (PCD) as cutting material. The PCD (90% diamond, 10% cobalt) was brazed to a cemented carbide substrate. The geometry of the indexable inserts and the cutting parameters are listed in Table 1.

Table 1. Machining conditions

Tool geometry (DCMT 11T304)			
Clearance angle: 7°	Tool cutting edge angle: 93°		
Rake angle: 0°	Tool cutting edge inclination: 0°		
Corner radius: 0.4 mm	Cutting edge radius: 12 µm		
Cutting parameters			
Cutting speed [m/min]	$v_{c1} = 100$	$v_{c2} = 200$	$v_{c3} = 300$
Depth of cut [mm]	$a_{p1} = 0.5$	$a_{p2} = 0.9$	$a_{p3} = 1.5$
Feed [mm/rev.]	$f_1 = 0.1$	$f_2 = 0.2$	$f_3 = 0.3$

New tools were used prior to the formation of significant wear forms (width of flank wear land << 100 µm) in order to prevent an appreciable influence of wear on the results of machining. The material of the workpieces was the aluminum wrought alloy Al2024. The workpieces were clamped in a chuck and supported using the center of the tailstock (Figure 1).

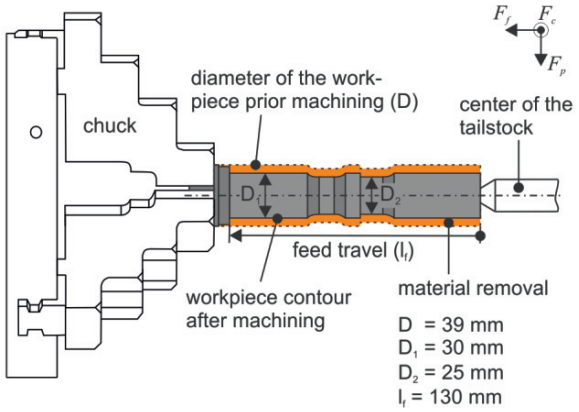

Fig. 1. Experimental setup

To analyze the effect of cutting conditions on the deformations of the workpiece during turning multiple characteristic values were determined. These are the forces, the diameter of the workpiece, the temperature distribution, and the heat flux into the workpiece. The process forces were measured using a three-component-dynamometer. The averages of the cutting force F_c, the feed force F_f, and the passive force F_p were calculated in order to evaluate the forces.

The temperature distribution in the workpiece was determined using three NiCr-Ni thermocouples (type K, wire diameter 1 mm). The position of the thermocouples varies regarding the direction of feed travel (Figure 2). Contrary to that, the radial position of the thermocouples is the same. Preliminary investigations revealed an insignificant temperature gradient in this direction. The workpiece undergoes an approximately homogenous radial heating.

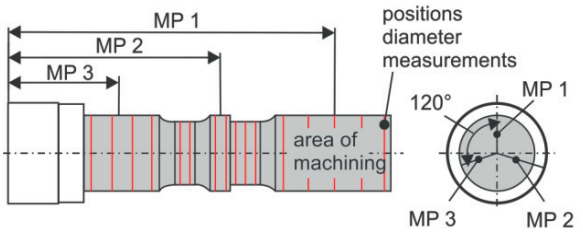

Fig. 2. Measurement positions (MP) of the thermocouples respectively the workpiece diameter

The quantity of heat (time integration of thermal power) at the workpiece Q_W was calculated according to

$$Q_W = mc(T_2 - T_1) \tag{1}$$

where m is the mass of the workpiece after the first tool engagement, c is the specific heat capacity of the material, T_2 is the average temperature of the workpiece after the first tool engagement, and T_1 is the workpiece temperature prior to turning. In order to determine T_2, the temperatures of the material were detected at each thermocouple position once the tool passed the respective position. The mean of these three temperatures was calculated to evaluate T_2. The heat flux $\dot{Q}_{in}$ into the workpiece is the result of the quantity of heat at the workpiece per time of an individual tool engagement t:

$$\dot{Q}_{in} = mc\frac{(T_2 - T_1)}{t} \tag{2}$$

The heat input into the workpiece when turning is approximately identical for each tool engagement in terms of a specific cutting condition. The heat input can therefore be determined at the first tool engagement in order to model the heat input for finite element simulations. Heat loss to the environment due to forced convection and heat conduction decreases the temperature of the workpiece. Heat radiation can be neglected because of the low workpiece temperatures and consequently small coefficients of emission. Taking the first tool engagement into account, heat loss is negligible. This can be attributed to the low temperature

difference between the workpiece and the environment. The use of multiple tool engagements requires the determination of thermal boundary conditions in order to capture the heat loss. As a result, coefficients of heat convection α_{cv} were determined as α_{cv}(v_c=100m/min) = 44 W/mK, α_{cv}(v_c=200m/min) = 62 W/mK, and α_{cv}(v_c=300m/min) = 80 W/mK. The coefficient of heat conduction αcd into the chuck was ascertained as α_{cd} = 1100 W/mK.

The diameter of the workpiece was measured at 16 positions inside of the feed travel by means of a 3D-coordinate-measuring-system (Figure 2). Using multiple measurement positions allows detecting possible differences of the diameter deviation in terms of the feed travel.

3. Finite Element Modeling

A FE model of the whole workpiece is used to calculate the temperature distribution in the workpiece, the related thermal expansion and the deflection of the workpiece due to the process forces.

The FE model inputs the heat flux into the workpiece, the forces and the coefficients of heat transfer as boundary conditions. These were experimentally determined. The magnitude of the heat flux and the process forces are approximately constant for a defined cutting condition. Measuring these loads once allows using them virtually for arbitrary workpiece geometries.

The rotational speed of the workpiece is remarkably higher than the feed velocity of the tool. The time for an individual revolution of the workpiece is therefore low, and consequently the feed travel during one revolution is small. Therefore, the heat flux into the workpiece Q_{in} can be assumed as axisymmetric when turning [11]. The rotational body forces are significantly minor than the cutting forces; they are negligible, and thus the rotation of the workpiece can be neglected too when simulating the deformations of the workpiece. The process forces act nonsymmetrical on the workpiece (Figure 3). The forces are actually producing alternating stresses, which are far below the yield strength of the workpiece material. They can therefore be assumed as static forces. The chuck is assumed as rigid restraint.

The temporal and local discretization of the heat flux, the process forces, and the removal of material needs to be determined in order to apply the loads on the workpiece in the chip formation area. Considering the removal of material allows for the calculation of the actual workpiece diameter after turning. The NC-code defines the location of the tool and therefore the chip formation area at each time increment. A preprocessor was written to numerically evaluate the NC-code by storing the coordinates of the tool positions regarding the respective time increments. Loads on the workpiece can thereby be applied nonstationary.

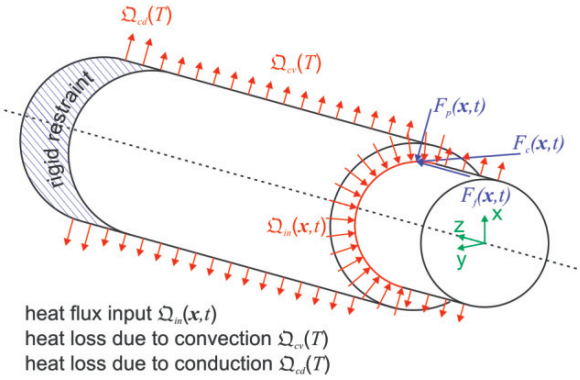

Fig. 3.Boundary conditions

To facilitate the removal of material the workpiece is meshed according to the respective tool paths. The removal of material and the mesh generation in 3D are performed axisymmetric. Therefore, first all nodes on the x-z-plane are defined and subsequently rotated around the z-axis. In this case cylindrical coordinates (r, θ, z) are suitable to define the mesh. In all regions to be machined, the maximum element edge length in r-direction matches the depth of cut. The element edge lengths in z-direction are defined according to an adequate depiction of the workpiece geometry. The number of elements around the circumference should be large enough to represent a circle in order to allow for an accurate determination of the workpiece deflection. The elements are structured in layers. This allows to arrange the element edges parallel to the direction of the tool path, see Figure 4.

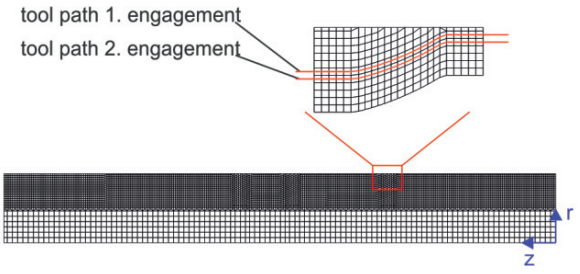

Fig. 4.Meshed workpiece in 2D at the x-z-plane

In the inner regions, which will be not machined, the element edge lengths are larger and not parallel to the direction of the tool path. Hex8 and Penta6 volume elements are used to discretize the workpiece geometry. The coordinates of the initial nodes are defined either approximately between subsequent tool paths, thus the tool path cuts approximately the midpoint of the element edges; or they are structured in equal distances across the workpiece (Figure 4). A preprocessor has been developed to generate the mesh evaluating the NC-code.

The removal of material is performed through the technique of element deactivation. The element edges do not fit the tool path because of the thermal expansion and the deflection of the workpiece. H-adaptive remeshing is required to perform the accurate removal of material. Thereby, each element is subdivided into eight new elements. The new nodes subdividing the old element in radial direction are positioned at the tool path and not as common in h-adaptive mesh refinement in the middle of the element edge or face. New nodes on the faces perpendicular to the radial direction can be positioned in the middle of the old element edges or faces (Figure 5). This allows an accurate removal of material.

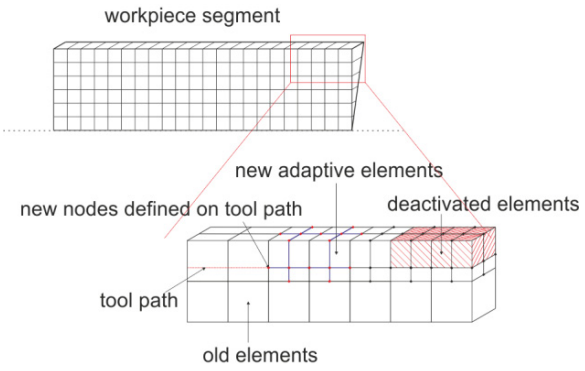

Fig. 5.Principle of remeshing and removal of material

Mesh refinement and element deactivation are done according to the NC-code. Each element is first refined and afterwards deactivated when the tool passes the respective position. The tool paths and the elements are defined prior to the FE-simulation. Using this information a user subroutine calculates the deactivation time for each element. The element refinement is carried out between two time steps and the element deactivation is done at the beginning of the time step. For this purpose the refinement time of each element is reduced by one time step.

In order to perform the heat flux into the workpiece and to apply the process forces each subdivided element is marked. In the next time step all marked and not deleted elements are subjected to the heat flux. The forces are only applied to the nodes of the newly refined elements, which were originally located on the x-z-plane. At the end of the time step these elements are marked to be the new workpiece surface. Thus the heat convection to the environment is continuously adapted according to the current workpiece surface.

To calculate the deflection of the workpiece, the center of the tailstock and the contact conditions in the center hole were modeled. The center of the tailstock rotates together with the workpiece during turning. The occurring relative displacement between the two bodies is due to deflection. Thermal and mechanical contact properties were considered when modeling the contact conditions.

Elastic properties are used to describe the mechanical behavior of the material. Table 2 shows the material properties of the aluminum alloy Al2024.

Table 2. Material properties Al 2024 [12]

Density ρ [kg/m³]	2780
E-modulus E [GPa]	73.0
Poisson's ratio ν	0.33
Dilation κ [µm/m°C]	0.00891 T + 22.2
Specific heat c [J/kg°C]	0.557 T + 877.6
Thermal conductivity	$T \leq 300$: 0.247 T + 114.4
λ [W/m°C]	$T > 300$: -0.125 T + 226.0

4. Results

To verify the finite element model, experimentally measured and simulated results have been compared for several cutting conditions. The results of one special cutting condition are depicted in the following. Remarkable differences between particular cutting conditions were experimentally observed in terms of the heat input, the maximum temperatures at the workpiece, and the deflection due to process forces. The deviations between simulated and measured values were nevertheless in the same percentage magnitude. The considered cutting condition possesses a cutting speed of v_c = 300 m/min, a feed of f = 0.3 mm/rev., and a depth of cut of a_p = 1.5 mm. The heat flux into the workpiece was determined as $\dot{Q}_{in}$ = 250 W, and the measured process forces as F_c = 435 N, F_f = 153 N, and F_p = 34 N.

Figure 6 shows the measured and calculated temperature in the workpiece at the three measurement positions (MP) as well as the temperature distribution on the surface for a particular tool position at the last tool engagement. The considered cutting condition exhibits three tool engagements. These are indicated by the peeks of the temperature at each measurement position. During the initial tool engagement the calculated temperatures fit the measured. At the last tool engagement deviations of up to 10% occur. These can be attributed to inaccuracies when determining the heat flux into the workpiece and heat loss due to assumptions respectively, e.g. a negligible heat loss to the environment at the first tool engagement. Regarding a defined tool engagement, the temperature deviation is the sum of the inaccuracies of each prior tool engagement. As a consequence, the deviation of the temperature values increases with the number of tool engagements.

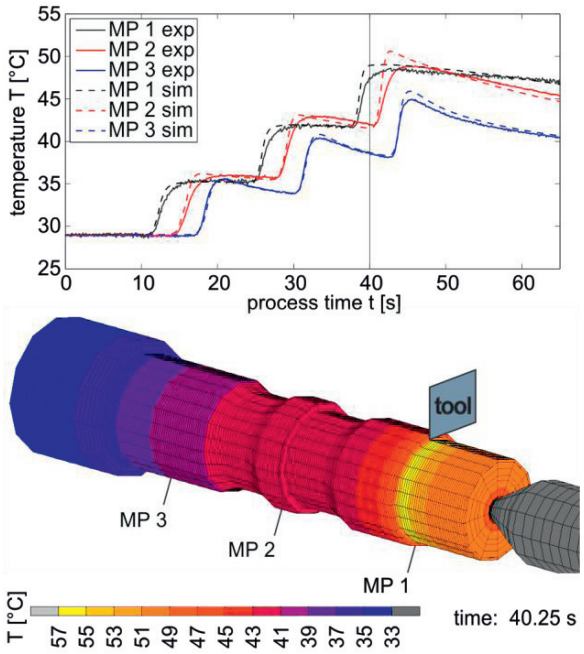

Fig. 6. Temperature distribution in the workpiece, complete machining process (top) and particular tool position (bottom)

The temperature of the workpiece rises at each tool engagement and declines during the time the tool is not in engagement. The remaining temperature increase between successive tool engagements at the initial stages of turning is greater than in the final stages. This can be ascribed to the greater heat loss between consecutive tool engagements at the final stages of turning due to the increasing temperature difference between the workpiece and the environment.

Figure 7 illustrates experimentally and numerically determined deviations from the nominal diameter regarding the feed travel. The experimentally measured deviations are predominantly caused by the thermal expansion of the tool and the workpiece as well as the deflections of workpiece and tool. Moreover, deviations occur due to the thermal expansion and the position accuracy of the machine tool. This research at present focuses on the simulation of the deformations of the workpiece.

The actual depth of cut is slightly decreased by the deflections of the workpiece at the actual tool position, especially in the vicinity of the tailstock center (Figure 7). Such deflections are affected by the stiffness of the machine tool-workpiece system, the length of the workpiece, the magnitude of the forces, and the arm of lever of the respective force. The lower the stiffness and the larger the forces, the arm of lever, and the length of the workpiece, the greater are the deflections. Consequently the greatest deflections, which decrease the actual depth of cut, are observed in the vicinity of the tailstock center.

The thermal expansions of the workpiece (Figure 7) are approximately in accordance with the determined temperature distribution in the workpiece (Figure 6). The lower the present temperatures, the smaller are the thermal expansions. The simulated and measured diameter deviations (Fig. 7) depict larger deviations at low feed travels l_f, where the temperature is higher during machining; compare MP1 (low l_f) and MP3 (high l_f) in Fig. 6. The green areas in Fig. 7 mark the regions of smaller nominal diameters. Since the thermal expansion depends on the dimension, the deviations are experimentally and numerically smaller in these regions. Experimentally measured deviations reveal a greater decrease in these areas than simulated deviations. Investigations of several cutting conditions (results of one are presented) showed a decrease in terms of diameter deviation from approximately 9 to 12 µm in these areas. Taking the observed temperature increases during turning into account, 1-4 µm of the decrease can be ascribed to the smaller thermal expansion of the material due to the smaller nominal workpiece diameter. The remaining, approximately constant, additional deviation of about 8 µm seems to be caused by the position accuracy and the interpolation technique (in order to manufacture the radius contour) of the lathe. These uncertainties may lead to a lathe induced difference between the nominal and the actual tool path when manufacturing the areas of smaller nominal diameter. The experimentally determined increase of the diameter deviation between the two green marked areas in Fig. 7 is hence also influenced. Such effects cannot be reproduced in the current model. For this purpose a model of the whole machine tool is needed [13].

For the present workpiece and cutting condition thermal effects are predominant; mechanical effects are indicated by the difference between the results of the two simulations in Fig. 7. Hence the diameter of the workpiece is undersized. The proportion of thermal and mechanical effects depends generally on the geometry and the material of the workpiece as well as on the cutting condition. In case of long and thin workpieces (particularly when cantilever mounted) mechanical effects are predominant.

The comparison of calculated and experimental results reveals numerically smaller deviations (Figure 7). The average of the measured deviations is approximately 22.6 µm. The simulated deviations possess a mean of approximately 11 µm. Uncertainties at the experimental investigations, such as the position accuracy of the machine tool or tool wear, affect the experimentally detected workpiece diameters. These uncertainties are indicated by the standard deviation in figure 7.

It is believed that in particular the thermal expansion of the tool and tool holder needs to be taken into account to further enhance the prediction of the actual workpiece diameter. In order to evaluate the magnitude of the thermal expansion of the tool for the considered cutting

condition, the temperature of the tool was measured during turning using thermocouples. These were positioned at the contact area between the indexable insert and the tool holder. A temperature increase during turning of 160 °C was observed. The thermal expansion of the tool can be estimated by equation (3)

$$\Delta l = \kappa_{\text{tool}} \Delta T l \tag{3}$$

to at least 8 µm. The actual depth of cut is accordingly increased. For the used indexable insert only the cemented carbide substrate has been considered for the estimation because it accounts for the biggest part of the tool mass. Its coefficient of dilation κ_{tool} is $5.0e^{-6}$ µm/m°C and the length l is 10 mm. Noteworthy contributions of the thermal expansion of the tool on the accuracy of machining were also revealed by other researchers [14, 15]. Taking the present deviation between experimental and numerical results into account, the consideration of tool deformations will remarkably enhance the prediction of the actual workpiece diameter. For this purpose separate FE models need to be used.

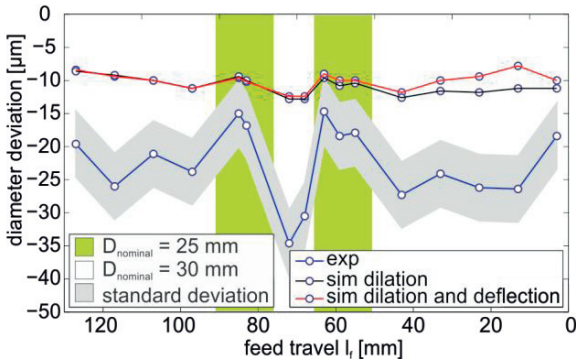

Fig. 7. Diameter deviation of the workpiece after machining

5. Conclusion And Outlook

The described method allows calculating the thermal expansion and the deflection of the workpiece. The heat flux into the workpiece, the process forces, and the coefficients of heat transfer are needed as boundary conditions. These were experimentally detected. The simulated temperature distribution in the workpiece fits the measured temperature values. Calculated diameter deviations are at present smaller than experimentally measured deviations. Numerically determined deviations comprise of the thermo-elastic expansion of the workpiece and the deflection due to the forces. In order to further enhance the prediction of the actual workpiece diameter, the thermal expansion and deflection of the tool and tool holder need to be taken into account. This can be carried out in a separate FE-model applying the thermal and mechanical loads on the tool.

Acknowledgements

The authors would like to thank the German research foundation (DFG) for funding the project "Thermal effects when turning Al-MMC - experiments and simulations AU 185/26, STE 544/42" within the priority program SPP 1480.

References

[1] Koch, K.F., 1996. Technologie des Hochpräzisions Hartdrehens, Dissertation, RWTH Aachen.
[2] Stephenson, D.A., Barone, M.R., Dargush, G.F., 1995. Thermal expansion of the workpiece in turning, Transactions of the ASME, Journal of Engineering for Industry 117/4, p. 542-550.
[3] Loehe, J., Zaeh, M.F., Roesch, O., 2012. In-process deformation measurement of thin-walled workpieces, Procedia CIRP 1, p. 563-568.
[4] Thoben, K.D., Lübben, T., Clausen, B. et al., 2002. Distortion engineering: Eine systemorientierte Betrachtung des Bauteilverzugs, Journal of Heat Treatment and Materials 57/4, p. 276–282.
[5] Sukaylo, V., Kaldos, A., Pieper, H.J. et al., 2005. Numerical simulation of thermally induced workpiece deformation in turning when using various cutting fluid applications, Journal of Materials Processing Technology 167/2-3, p. 408–414.
[6] Nicolai, M., Hegler, R., 1980. Werkstücktemperatureinfluss beim Drehen, VDI-Z Intergierte Produktion 6, p. 225–228.
[7] Bryan, J., 1997. International status of thermal error research, CIRP Annals - Manufacturing Technology 39/2, p. 645–656.
[8] Fleischer, J., Pabst, R., 2007. Heat flow simulation for dry machining of power train castings, CIRP Annals - Manufacturing Technology 56/1, p. 117–122.
[9] Bana, V., Karpuschewski, B., Kundrak, J. et al., 2007. Thermal distortions in the machining of small bores, Journal of Materials Processing Technology 191/1-3, p. 335–338.
[10] Tai, B.L., Jessop, A.J., Stephenson, D.A., Shih, A.J., 2012. Workpiece thermal distortion in minimum quantity lubrication deep hole drilling – finite element modeling and experimental validation, Journal of Manufacturing Science and Engineering 134/1, p. 1-9.
[11] Sukaylo, V., 2003, Numerische Simulation der thermisch bedingten Werkstückabweichungen beim Drehen mit unterschiedlichen Kühlschmiermethoden, Dissertation, Otto-von-Guericke-Universität Magdeburg.
[12] Asad, M., Girardin, M., Mabrouki, T., Rigal, J.-F., 2008. Dry cutting study of an aluminium alloy (a2024-t351): a numerical and experimental approach, International Journal of Material Forming 1, p. 499–502.13
[13] Schwarz, F., 2010. Simulation der Wechselwirkung zwischen Prozess und Struktur bei der Drehbearbeitung, Dissertation, TU München.
[14] Moriwaki, T., Horiuchi, A., Okuda, K., 1990. Effect of cutting heat on machining accuracy in ultra-precision diamond turning, CIRP-Annals - Manufacturing Technology 39/1, p. 81-84.
[15] Zhou, J.M., Anderson, M., Stahl, J.E., 2004. Identification of cutting errors in precision hard turning process, Journal of Materials Processing Technology 153-154, p. 746-750.